Optimal Preventive Strategies for Transient Voltage Stability with Grid-Forming Wind Integration

Behzad Heydari
Electrical Engineering Department
Université Laval
Québec, Canada
behzad.heydari.1@ulaval.ca

Seyed Masoud Mohseni-Bonab
Hydro-Québec
75, boulevard René-Lévesque Ouest
Montréal, Québec, Canada
s.m.mohsenibonab@ieee.org

Innocent Kamwa
Electrical Engineering Department
Université Laval
Québec, Canada
innocent.kamwa@gel.ulaval.ca

***Abstract*— This paper presents a two-step preventive algorithm to mitigate the risk of transient voltage instability (TVI). The core idea is to proactively use generation rescheduling (GR) and demand response (DR) to lessen the impact of line contingencies with the potential for causing TVI. In the first step, contingency analysis is performed on a modified IEEE 39-bus system with grid-forming (GFM) wind turbines (WTs) using time-domain simulation (TDS) to assess how likely outage of various lines are to cause TVI for an upcoming operating point. Hence, critical and quasi-critical lines, along with their critical loadings, are identified. In the second step, these critical loadings are treated as security constraints in an optimization process. The algorithm then determines the optimal value of DR and GR to keep the system stable by reducing the loading on the risky lines. The procedure iterates until a secure operating point is reached. A key contribution is the coordinated, optimization-based use of GR and DR with explicit assessment of wind participation in rescheduling. Two scenarios are studied: Scenario I fix wind output, while Scenario II allows GFM wind to participate in GR with bounded curtailment. Case studies show that Scenario II achieves higher time-to-voltage-collapse (TVC) and lower operating costs than the fixed-wind baseline in Scenario I, demonstrating that treating GFM wind as a controllable resource mitigates TVI, while reducing operational expenditure.**

***Index Terms*—Transient Voltage Stability, Wind Energy, Generation Rescheduling, Demand Response.**

I. Introduction

Transient Voltage Stability (TVS) is essential for secure power-system operation. Transient Voltage Instability (TVI) arises when the voltage stability margin is insufficient after a disturbance [1]. To evaluate such phenomena, time domain simulations (TDS) are commonly employed because they capture the combined effects of fast acting devices such as induction motor loads (IMLs), and slow acting components, including under load tap changers (ULTCs) and over excitation limiters (OELs). IMLs, which is common in air conditioning and other motor driven loads, exhibit high reactive power during faults, often causing Fault-Induced Delayed Voltage Recovery (FIDVR) and potentially voltage collapse if not properly mitigated [2].

In today's power systems, the growing penetration of inverter-based resources (IBRs) has significantly altered system dynamics, making it essential to account for their behavior in stability analyses. IBRs are typically classified as grid-following (GFL) or grid-forming (GFM) according to their control philosophy and grid interaction. Ref. [3] provides a comparative study showing that GFM controllers offer superior frequency and transient performance, especially under weak grids, although their explicit influence on voltage stability remains insufficiently investigated. This aligns with [4] which analyzes the dynamic interactions of GFL and GFM inverters under decentralized coordination and emphasizes the need to include GFM in dynamic stability assessments. TVS enhancement strategies fall into device-based and operational preventive or corrective actions. Device-based methods such as installing additional reactive support or advanced converters can be effective but often require substantial capital investment and infrastructure upgrades. In contrast, operational strategies, generation rescheduling (GR), demand response (DR), and real-time control schemes, are more flexible and cost-effective. Ref. [5] integrates voltage and transient stabilities in a multi-objective OPF, thereby improving margins and cost; [6] proposes a remedial scheme combining GR, load shedding, and ULTC blocking for mid- and long-term voltage instability.

Recent studies have explored various techniques for mitigating TVI; however, the influence of renewable energy resources and the dynamic behavior of OELs, ULTCs, and IMLs have rarely been examined through TDS. In [7], PSO is applied to tune the PID parameters of AVRs in synchronous generators to improve voltage regulation, but remains limited to conventional generator-based grids and neglects IBR interactions. Also, a rule-based algorithm is proposed in [8] that ensures cyber-resilient grid monitoring. This study explicitly considers OELs and ULTC to capture long-term voltage stability effects, but is limited to load-restoration scenarios and ULTC blocking mitigation. Meanwhile, [9] develops a decision-tree framework for TVS prediction from real-time data, yet it omits OEL-ULTC interactions. A learning-based method that detects voltage instability and mitigates it via selective ULTC blocking is also introduced in [10]; nevertheless, most such methods still do not capture the dynamic interactions of GFM inverters with other grid components. Model-based emergency load shedding strategies have also been proposed in [11], but the absence of OELs, ULTCs, and GFM dynamics limits their relevance to modern networks. In addition, distributed DR-based optimal power flow has been explored in [12], while other data-driven methods such as ensemble sparse oblique regression trees [13] and time-series forecasting [14] have been used to extract voltage-stability operating rules but often overlook nonlinear, transient IBR effects. Likewise, industrial-specific solutions (e.g., electrolytic aluminum load management [15]) and machine learning-based emergency assessment with load shedding [16] underutilize renewable participation. Other efforts, including load-shedding-based remedial schemes [17], CNN-based preventive controls [18], and day-ahead unit-commitment formulations with TVS constraints [19], mainly target conventional or GFL resources and do not explicitly capture fast IBR/GFM dynamics.

Motivated by these gaps, this study proposes an operational, preventive framework that coordinates GR, DR, and wind turbines (WTs) with GFM controllers under explicit dynamic

979-8-3315-8138-1

TVS constraints. Unlike prior work that neglects ULTCs and OELs or treats only one, the method simultaneously models both—together with IML dynamics—in TDS to capture the relevant transient behavior. It also simultaneously utilizes DR and GR as operational actions without additional control devices like FACTS, mitigating TVI risk in advance at a given operating point ($t + \Delta t$). Two scenarios are considered: (i) GFM wind at fixed output without curtailment and (ii) GFM wind participating in GR with bounded curtailment. This dual-scenario enables a comprehensive assessment of GFM-based renewable contribution to TVI mitigation. The approach iteratively enforces line-specific critical loadings (P_k^{CL}) to drive the system toward a TVS-secure operating point.

II. THE PROPOSED APRROACH

In power systems, the outage of transmission lines occurs commonly due to faults, adverse weather conditions, or maintenance operations. Such outages are considered critical contingencies because they can redistribute power flows, overload adjacent lines, and induce voltage deviations across the network. For a power system supplying IMLs and incorporating devices such as ULTCs and OELs, the outage of a transmission line can, depending on its location and the system's pre-outage operating condition, cause a TVI that may ultimately lead to voltage collapse. To mitigate these effects, GR is a robust and effective approach for managing the overloads on adjacent lines following the outage of a line [20]. In addition, DR programs provide a practical means to further reduce such overloads by temporarily adjusting consumer demand. Hence, this paper investigates the combined effectiveness of GR and DR programs in alleviating line overloading resulting from the outage of lines for an upcoming operating point ($t + \Delta t$). From a TVS perspective, if the outage of a line causes the system to undergo TVI, that line is labeled as a critical line. Each critical line has a corresponding critical loading (P_k^{CL}), which is lower than its current loading level (P_k^L) (i.e., $P_k^{CL} \leq P_k^L$). However, when the loading of critical lines is reduced, other lines may approach or exceed their own loading limits, potentially becoming critical themselves. To address this, quasi-critical lines are defined as lines whose outages do not directly trigger TVI but whose current loading is close to their critical loading threshold. Specifically, when the loading of a non-critical line approaches a predefined fraction (λ) of its critical loading ($P_k^L > \lambda \times P_k^{CL}$, with $\lambda = 0.9$), such lines are labeled as quasi-critical. This classification helps prevent secondary overloads during the process of mitigating stress on the initially critical lines. The procedures for determining P_k^{CL} are as follows:

- For a critical line k: Decrease the system load–generation level simultaneously in steps of $\partial P = 5\%$. At each step, simulate the outage of line k. The highest loading level at which the outage no longer causes TVI is taken as P_k^{CL}.
- For a quasi-critical line k: Increase the system load–generation simultaneously level in steps of $\partial P = 5\%$. At each step, simulate the outage of line k. The lowest loading level at which TVI first appears is taken as P_k^{CL}.

To alleviate the overloading of critical lines while preventing additional stress on quasi-critical lines, a coordinated optimization of GR and DR is employed. The proposed two-step algorithm operates as follows. Step 1 identifies critical ($\mathcal{C}$) and quasi-critical ($\mathcal{Q}$) lines and determines their corresponding TVC and critical loading values (P_k^{CL}). Step 2 incorporates P_k^{CL} as security constraints in a cost-minimizing program that co-optimizes GR, DR, and in Scenario II, GFM-wind curtailment. Solving this optimization problem relieves the loading of critical lines and increases TVC, thereby mitigating TVI risk. The procedure iterates between Step 1 and Step 2 until convergence to a TVS-secure operating point. Algorithm 1 summarizes the overall method.

ALGORITHM I. THE ALGORITHM OF THE PROPOSED METHOD

Preliminaries (Operating Point at $t + \Delta t$)

Forecast the load at $t + \Delta t$; and ***set*** initial operating point

Configure wind-turbine scenarios:

- ***Scenario I:*** Two GFM WTs fixed at 200 MW each (no curtailment).
- ***Scenario II:*** Two GFM WTs curtailable with $k = 0.25$.

Initialize $iter = 1$, $\varepsilon^* = 0.01$, and $\lambda = 0.9$.

Step 1 – Identification of Critical ($\mathcal{C}$) and Quasi-Critical ($\mathcal{Q}$) lines and their critical-loadings (P_k^{CL})

for each line $k \in \{1, \dots, N_L\}$ ***do***
  Run Load Flow
  Record current loading of line $P_k^{L^V}$; where $V \leftarrow 0$
  RMS Simulation for TVI studies by the outage of line k.
  If there is TVI ***do***
    Label Critical, and ***Compute*** TVC_k .
    While there is TVI ***do***
      Decrease load–generation by $\partial P = 5\%$, and ***Set*** $V \leftarrow V + 1$
      RMS Simulation for TVI studies by the outage of line k
    End While
    Set $P_k^{CL} \leftarrow P_k^{L^V}$ and ***Continue***.
  Else
    While there isn't TVI ***do***
      Increase load–generation by $\partial P = 5\%$, and ***Set*** $V \leftarrow V + 1$
      RMS Simulation for TVI studies by the outage of line k
    End While
    If $P_k^{L^0} > \lambda \times P_k^{L^V}$ **do**
      Set $P_k^{CL} \leftarrow P_k^{L^V}$
      Label Quasi-critical, ***Compute*** TVC_k , and ***Continue***.
    Else ***Label*** Safe.
End for
Collect Sets $\boldsymbol{\mathcal{C}}$ and $\boldsymbol{\mathcal{Q}}$ and their $\{\boldsymbol{P_k^{CL}}, \boldsymbol{TVC_k}\}$

Step 2 – Optimization (GR + DR + WT Curtailment)

Formulate an NLP, where:

Objective function:

$$min\ OF = Cost^{total} = Cost_{GR} + Cost_{WT} + Cost_{DR}$$

Subject to: equations (3-18), (20), and:

$$P_k^L \leq P_k^{CL} \qquad (\forall k \in \boldsymbol{\mathcal{C}}\ and\ \boldsymbol{\mathcal{Q}}).$$

Solve with Pyomo package on Python

Convergence and Repeat

Compute: $\varepsilon_k = \frac{(P_k^L - P_k^{CL})}{P_k^L}$ for all $k \in \mathcal{C}$.

If $max_{k \in \mathcal{C}}\ \varepsilon_k \leq \varepsilon^*$ ***do***
  Return a TVS-secure operating point for $t + \Delta t$ and ***Exit***
Else
  Set $iter \leftarrow iter + 1$; and ***Return to*** Step 1.

The optimization problem used in the second step is formulated as follows:

979-8-3315-8138-1

$$min \qquad Cost^{total} = Cost_{GR} + Cost_{WT} + Cost_{DR} \tag{1}$$

$$Cost_{GR} = W_{GR}\left(\sum_{i=1}^{N_G} a_i \times \left(\Delta P_i^G\right)^2 + b_i \times \left|\Delta P_i^G\right|\right)$$

$$Cost_{WT} = W_{WT}\left(\sum_{i=1}^{N_{WT}} \sigma_i \times \Delta P_i^{WT}\right)$$

$$Cost_{DR} = W_{DR}\left(\sum_{d=1}^{N_D} \alpha_d \times \left(\Delta P_d^D\right)^2 + \beta_d \times \left(\Delta P_d^D\right)\right)$$

$$W_{GR} + W_{WT} + W_{DR} = 1 \tag{2}$$

$$P_i^G + P_i^{WT} - P_i^D = \sum_{j=1}^{NB} P_{ij}^L \tag{3}$$

$$P_{ij}^L = \left(\frac{{V_i}^2}{Z_{ij}} cos(\theta_{ij}) - \frac{V_i \times V_j}{Z_{ij}} cos\left(\delta_i - \delta_j + \theta_{ij}\right)\right) \tag{4}$$

$$Q_i^G + Q_i^{WT} - Q_i^D = \sum_{j=1}^{NB} Q_{ij}^L \tag{5}$$

$$Q_{ij}^L = \left(\frac{{V_i}^2}{Z_{ij}} \sin(\theta_{ij}) - \frac{V_i V_j}{Z_{ij}} \sin\left(\delta_i - \delta_j + \theta_{ij}\right) - \frac{b_{ij}{V_i}^2}{2}\right) \tag{6}$$

$$P_i^G = {P_i^G}^0 + \Delta P_i^G \tag{7}$$

$$P_d^D = {P_d^D}^0 - \Delta P_d^D \tag{8}$$

$$Q_d^D = P_d^D \times \tan(\phi_d^D) \tag{9}$$

$$\underline{V_i} \leq V_i \leq \overline{V_i} \tag{10}$$

$$\underline{P_i^G} \leq P_i^G \leq \overline{P_i^G} \tag{11}$$

$$-\overline{\Delta P_i^G} \leq \Delta P_i^G \leq \overline{\Delta P_i^G} \tag{12}$$

$$\underline{Q_i^G} \leq Q_i^G \leq \overline{Q_i^G} \tag{13}$$

$$\Delta P_d^D \geq 0 \tag{14}$$

$$0 \leq P_i^{WT} \leq \overline{P_i^{WT}} \tag{15}$$

$$\Delta P_i^{WT} = \overline{P_i^{WT}} - P_i^{WT} \tag{16}$$

$$0 \leq \Delta P_i^{WT} \leq k^{cur} \times \overline{P_i^{WT}} \tag{17}$$

$$-\tan(\varphi_{lead}) \times P_i^{WT} \leq Q_i^{WT} \leq \tan(\varphi_{lag}) \times P_i^{WT} \tag{18}$$

$$P_{ij}^L \leq P_{ij}^{CL} \qquad ; if \;\; P_{ij}^{CL} < \overline{P_{ij}^L} \qquad \forall\, ij \in \mathcal{C} \,\&\, \mathcal{Q} \tag{19}$$

$$P_{ij}^L \leq \overline{P_{ij}^L} \qquad \forall\, ij \notin \mathcal{C} \,\&\, \mathcal{Q} \tag{20}$$

Eq. (1) minimizes total operating cost as a weighted sum of GR, WT curtailment, and DR costs, with weights W_{GR} ,W_{WT}, and W_{DR} satisfying Eq. (2). The GR cost uses generator-specific coefficients a_i/b_i; the WT curtailment cost uses σ_i; and the DR cost uses load-specific coefficients α_d/β_d. Eqs. (3)-(6) impose active/reactive power flow balances. Eqs. (7)-(9) define GR and DR adjustments at buses. Eqs. (10)-(14) enforce voltage limits, generator P/Q limits, rescheduling bounds, and nonnegativity of DR. Eq. (15) limits injected wind power (P_i^{WT}) by available wind ($\overline{P_i^{WT}}$). Eq. (16) defines curtailment (ΔP_i^{WT}) as the gap between available and injected wind. Eq. (17) bounds curtailment to a fixed fraction ($k = 0.25$) of availability. Eq. (18) constrains the reactive power of the WTs (Q_i^{WT}). Eq. (19) enforces line security using the proposed critical loadings (P_{ij}^{CL}) for critical/quasi-critical. Eq. (20) applies thermal flow limits ($\overline{P_{ij}^L}$) to the remaining (safe) lines.

An optimal operating point with minimal or no risk of TVI is obtained by solving the formulated optimization problem. However, due to the inherent nonlinearity of power systems with respect to voltage stability—and the dependence of each line's critical loading on the system's operating condition—the optimization problem cannot satisfy all line constraints in only one iteration. This is because changes in the operating point alter the critical loadings of the lines, which in turn affect the optimal solution. To handle this dependency, an iterative solution approach is employed. The process continues until a convergence criterion is met for all critical lines, defined as:

$$\varepsilon_{ij} = \frac{P_{ij}^L - P_{ij}^{CL}}{P_{ij}^L} \leq 0.01 \tag{21}$$

Convergence (e.g., $\varepsilon_{ij} = 0.009$ for all lines) indicates P_{ij}^L and P_{ij}^{CL} have nearly matched within tolerance. During each iteration, loadings shrink while TVCs increase, demonstrating mitigated TVI. If some lines remain critical at the final solution, the available controls are insufficient for full remediation and post-contingency corrective actions might be required.

III. Simulation Results

The effectiveness of the proposed method is evaluated on a modified IEEE 39-bus system (345 kV), a standard benchmark for dynamic-stability studies, which is shown in Fig. 1. Time-domain simulations for TVI assessment and critical loading evaluation of critical and quasi-critical lines are performed in PowerFactory®. The optimization problem is formulated as a Nonlinear Programming (NLP) model and solved using the IPOPT solver within the Pyomo framework on Python, ensuring an optimal balance between GR and DR while maintaining system feasibility. The network comprises 47 buses, 10 synchronous generating units, 34 transmission lines, and two GFM WTs, each rated 200 MW. The system includes six IMLs (883 MW, 748 MVAR) connected through ULTC-equipped transformers; all generators employ OELs. Non-motor loads fully participate in DR. A system loading of 4578 MW is used for performance evaluation, with bus 39 as the reference.

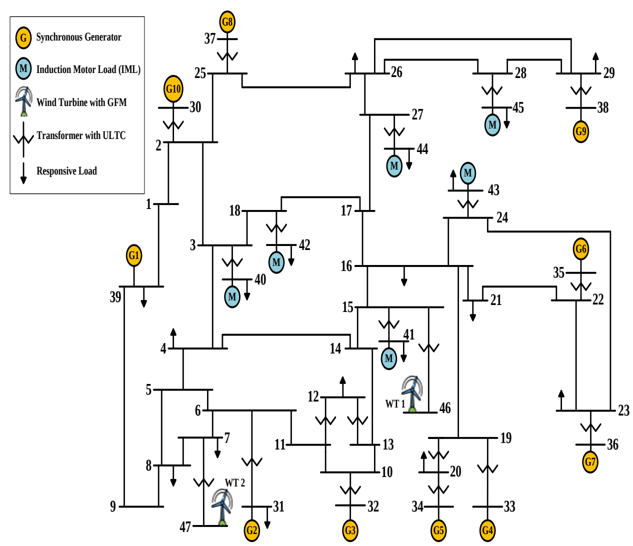

Figure 1. Single line diagram of modified IEEE 39-bus system

A. Scenario I- Without Wind Participation

The WT1 and WT2 are excluded from generation redispatch, therefore their outputs remain fixed at 200 MW across all five iterations. Fig. 2 shows the voltage behavior at bus 15 following the outage of a critical line 15-14 over successive iterations. TVC increases from 71 second to 258 second after iteration 5, which evidences progressive mitigation of TVI.

979-8-3315-8138-1

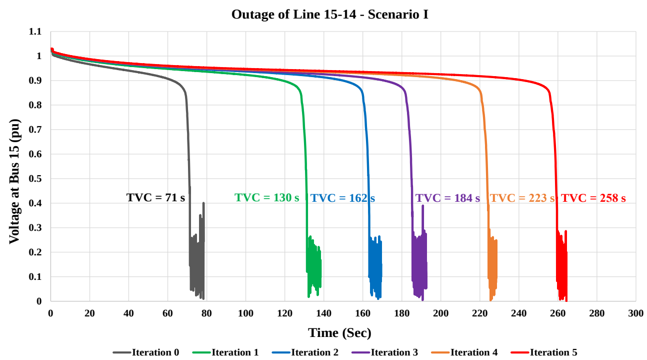

Figure 2. Voltage at bus 15 following the outage of line 15-14 –Scenario I

Table I summarizes the stability status for all critical lines, indicating their TVCs in seconds. Prior to applying the proposed algorithm, 19 lines are critical and the remaining 15 are quasi-critical (i.e., no line is initially safe). After five iterations, 14 lines are fully cleared (TVC = ∞) and only five critical lines remain, but with an enhancement in their TVC values. This provides operators more time to implement corrective actions in post-contingency mode.

TABLE I. THE TVI STATUS OF ALL CRITICAL LINES – SCENARIO I

Critical Line	PL (MW)	Without Wind participation					
		Iter. 0	Iter. 1	Iter. 2	Iter. 3	Iter. 4	Iter. 5
		TVC(s)	TVC(s)	TVC(s)	TVC(s)	TVC(s)	TVC(s)
02-01	174	35	71	109	144	207	∞
03-02	-390	37	60	77	88	104	122
04-03	-24	127	∞	∞	∞	∞	∞
05-04	142	116	∞	∞	∞	∞	∞
09-08	-74	207	∞	∞	∞	∞	∞
14-13	-216	187	∞	∞	∞	∞	∞
15-14	-41	71	130	162	184	223	258
17-16	-150	35	∞	∞	∞	∞	∞
18-03	-88	84	∞	∞	∞	∞	∞
21-16	187	140	∞	∞	∞	∞	∞
22-21	375	43	91	145	249	∞	∞
24-23	-220	95	∞	∞	∞	∞	∞
25-02	62	50	∞	∞	∞	∞	∞
26-25	-110	18	39	59	77	111	159
27-17	-20	23	125	∞	∞	∞	∞
28-26	85	10	16	21	25	30	36
29-26	132	10	18	24	29	38	48
29-28	272	20	51	91	177	∞	∞
39-01	-173	81	∞	∞	∞	∞	∞

The Fig. 3 summarizes the GR participation across all units. As shown, the two WTs undergo no curtailment in this scenario. It is also noteworthy that the economic cost coefficients are unit-specific, where each generator has distinct (a_i, b_i) parameters in Eq. (1) with no two units sharing identical values.

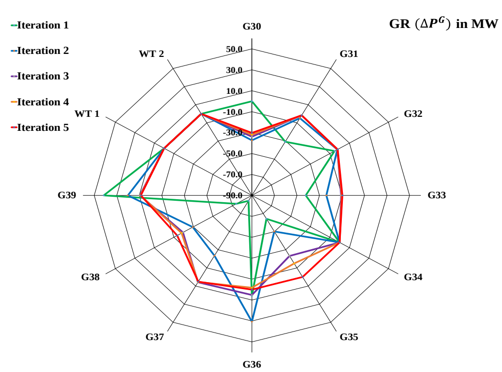

Figure 3. The GR contribution without WTs participation –Scenario I

Fig. 4 presents the DR outcomes at the responsive load buses for Scenario I, which depict the MW participation at each responsive bus across five iterations. The response is spatially selective: bus 41 provides the largest contribution, with a cumulative 104.8 MW of shedding load, whereas many buses remain near zero. Additional load shedding is concentrated at buses 44, 40, 26, 42, 21, 43, 45, and 20 indicating that the scheme targets electrically influential locations rather than distributing DR uniformly.

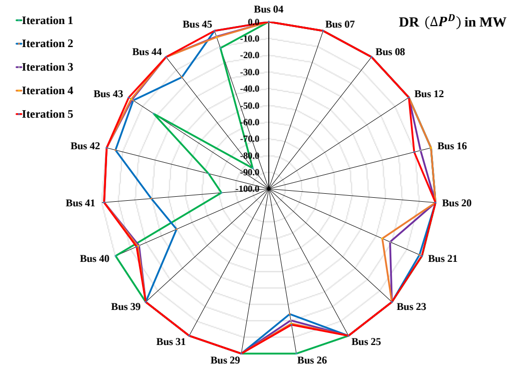

Figure 4. The DR contribution graph through 5 iterations –Scenario I

B. *Scenario II- With Wind Participation*

In this scenario, the GFM WTs at buses 46 and 47 are allowed to participate in GR alongside the conventional units. As Fig. 5 shows the voltage at bus 15 following the outage of line 15–14, the TVC increases monotonically, from 71 seconds at the baseline to 156 seconds at iteration 1, 199 seconds at iteration 2, and 247 seconds at iteration 3. From iteration 4 onward, the voltage no longer collapses (TVC = ∞). In practical terms, enabling GFM WTs participation progressively improves TVS and clearly outperforms Scenario I, where wind output was fixed.

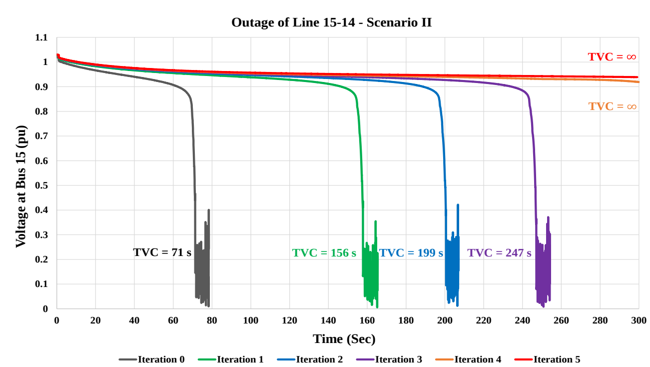

Figure 5. Voltage at bus 15 following the outage of line 15-14 –Scenario II

The resulting TVI outcomes are reported in Table II. Across all critical lines and all iterations, the TVCs are consistently higher than in Scenario I, indicating a better improvement in TVS when wind participates in the generation redispatch. As an example, line 22-21 is resolved after three iterations in Scenario II, whereas four iterations were required in Scenario I. This demonstrates that coordinated rescheduling including GFM wind accelerates convergence to a secure operating point and enhances post-contingency voltage robustness.

Fig. 6 illustrates the GR contribution across all generating units when GFM WTs are allowed to participate in the

979-8-3315-8138-1

rescheduling process. In contrast to Scenario I, wind adjustments are non-zero: WT2 provides a cumulative -34.4 MW curtailment over the five iterations. Economically, Scenario II achieves lower operating expenditures compared to Scenario I, with the GR and DR cost components decreasing by 5.9 % and 4.6 %, respectively. Moreover, the participation of GFM-based WTs enhances the overall system performance by providing a greater mitigation in TVI, confirming the combined benefits of lower cost and improved voltage stability.

TABLE II. THE TVI STATUS OF ALL CRITICAL LINES – SCENARIO II

Critical Line	PL (MW)	With Wind participation					
		Iter. 0	Iter. 1	Iter. 2	Iter. 3	Iter. 4	Iter. 5
		TVC(s)	TVC(s)	TVC(s)	TVC(s)	TVC(s)	TVC(s)
02-01	174	36	79	119	162	243	∞
03-02	-390	37	63	8	94	110	130
04-03	-24	127	∞	∞	∞	∞	∞
05-04	142	116	∞	∞	∞	∞	∞
09-08	-74	207	∞	∞	∞	∞	∞
14-13	-216	187	∞	∞	∞	∞	∞
15-14	-41	71	156	199	247	∞	∞
17-16	-150	35	∞	∞	∞	∞	∞
18-03	-88	84	∞	∞	∞	∞	∞
21-16	187	140	∞	∞	∞	∞	∞
22-21	375	43	104	178	∞	∞	∞
24-23	-220	95	∞	∞	∞	∞	∞
25-02	62	50	∞	∞	∞	∞	∞
26-25	-110	18	42	65	88	133	203
27-17	-20	23	186	∞	∞	∞	∞
28-26	85	10	17	22	26	33	40
29-26	132	10	18	25	31	41	54
29-28	272	20	56	105	242	∞	∞
39-01	-173	81	∞	∞	∞	∞	∞

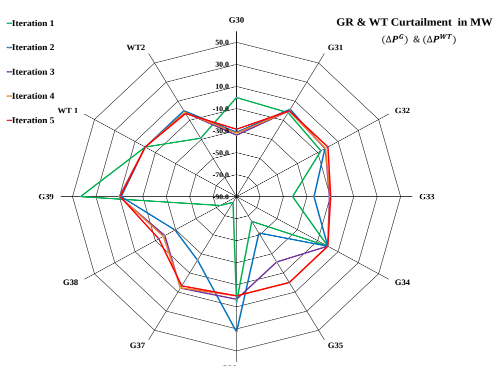

Figure 6. The GR contribution with WTs participation –Scenario II

IV. CONCLUSION

This paper presented a two-step preventive algorithm that couples TDS-based contingency screening with a cost-minimizing GR/DR optimization subject to line-specific critical-loading security constraints. In Step 1, TDS on the modified IEEE 39-bus system with GFM WTs identified critical and quasi-critical lines and their critical loadings. In Step 2, these limits were enforced within the optimization. By iterating the two steps, the system converges to a TVS-secure operating point. Case studies on the IEEE 39-bus system show that enabling GFM wind participation in rescheduling speeds convergence to a secure operating point (i.e., raising TVCs, clearing more critical lines, and lowering operating costs). These results indicate that treating GFM WT as a controllable resource enhances post-contingency voltage robustness while curbing operational expenditure. When residual critical lines remain after some iterations, fully clearing them in the preventive mode would require additional GR/DR cost; however, the increased TVCs give operators more time to apply post-contingency corrective actions.

REFERENCES

[1] N. Hatziargyriou *et al.*, "Definition and classification of power system stability–revisited & extended," *IEEE Transactions on Power Systems*, vol. 36, no. 4, pp. 3271-3281, 2020.
[2] C. Liu *et al.*, "Online voltage stability assessment for load areas based on the holomorphic embedding method," *IEEE Transactions on Power Systems*, vol. 33, no. 4, pp. 3720-3734, 2017.
[3] S. Yari, I. Kamwa, and D. Rimorov, "Comparison of Grid-Following and Grid-Forming Inverters Performance for Frequency Stability in Power Systems: A Dynamic Study," in *2024 IEEE Canadian Conference on Electrical and Computer Engineering (CCECE)*, 2024: IEEE, pp. 363-368.
[4] R. Debnath, A. Umar, G. S. Gupta, D. Kumar, I. Kamwa, and P. K. Jamwal, "Dynamical Stability Analysis of Grid-Following and Grid-Forming Inverters With Blockchain Integration for Enhanced Performance in Modernized Nested Microgrids," *IEEE Access*, vol. 13, pp. 165769-165794, 2025.
[5] S. Hashemi *et al*, "An integrated approach for incorporation of voltage and transient stabilities into optimal power flow study," *Electric Power Systems Research*, vol. 206, p. 107784, 2022.
[6] H. Khoshkhoo *et al*, "A remedial action scheme to prevent mid/long-term voltage instabilities," *IEEE Systems Journal*, vol. 15, no. 1, pp. 923-934, 2020.
[7] H. Zimmer, B. Niersbach, and J. Hanson, "Optimization of power plant AVR parameters to improve transient voltage stability," in *2017 11th IEEE International Conference on Compatibility, Power Electronics and Power Engineering (CPE-POWERENG)*, 2017: IEEE, pp. 71-76.
[8] M. Khalilifar and S. M. Shahrtash, "Early Detection of Voltage Instability: A Transparent, Rule-Based Method for Cyber-Resilient Grids," *IEEE Access*, vol. 13, pp. 142262-142273, 2025.
[9] M. Lashgari and S. M. Shahrtash, "Fast online decision tree-based scheme for predicting transient and short-term voltage stability status and determining driving force of instability," *International Journal of Electrical Power & Energy Systems*, vol. 137, p. 107738, 2022.
[10]F. K. Alabbas *et al.*, "A Novel Data Driven Model for Voltage Stability Status Prediction and Instability Mitigation," *International Transactions on Electrical Energy Systems*, vol. 2025, no. 1, p. 6575682, 2025.
[11]Y. Dong *et al.*, "An emergency-demand-response based under speed load shedding scheme to improve short-term voltage stability," *IEEE Transactions on Power Systems*, vol. 32, no. 5, pp. 3726-3735, 2017.
[12]Y. Dong, X. Xie, W. Shi, B. Zhou, and Q. Jiang, "Demand-response-based distributed preventive control to improve short-term voltage stability," *IEEE Transactions on Smart Grid*, vol. 9, no. 5, pp. 4785-4795, 2017.
[13]H. Jia *et al.*, "Voltage stability constrained operation optimization: An ensemble sparse oblique regression tree method," *IEEE Transactions on Power Systems*, vol. 39, no. 1, pp. 160-171, 2023.
[14]M. Taheri *et al.*, "A novel centralized load shedding approach to assess short-term voltage stability: a model-free using time series forecasting," *IEEE Transactions on Power Delivery*, vol. 38, no. 5, pp. 3076-3083, 2023.
[15]S. Liao *et al.*, "Emergency Control Strategy for Electrolytic Aluminum Load Considering the Load's Transient Overcurrent Characteristics and Transient Voltage Stability Constraints," *IEEE Transactions on Power Systems*, vol. 40, no. 2, pp. 1699-1711, 2024.
[16]Z. Zhang *et al*, "SE-CNN based emergency control coordination strategy against voltage instability in multi-infeed hybrid AC/DC systems," *International Journal of Electrical Power & Energy Systems*, vol. 160, p. 110082, 2024.
[17]M. Sarwar *et al.*, "Short-term Voltage Stability Improvement in Power System through Grid-forming Hybrid PV Plants," *IEEE Transactions on Industry Applications*, vol. 61, no. 5, pp. 7892-7902, 2025.
[18]Z. Li, J. *et al.*, "Preventive control method of improving transient voltage stability for power system based on the attention of CNN," in *2023 IEEE Sustainable Power and Energy Conference (iSPEC)*, 2023: IEEE, pp. 1-5.
[19]M. Jiang *et al.*, "Short-term voltage stability-constrained unit commitment for receiving-end grid with multi-infeed HVDCs," *IEEE Transactions on Power Systems*, vol. 36, no. 3, pp. 2603-2613, 2020.
[20]L. Lenoir, I. Kamwa, and L.-A. Dessaint, "Overload alleviation with preventive-corrective static security using fuzzy logic," *IEEE Transactions on Power Systems*, vol. 24, no. 1, pp. 134-145, 2009.

979-8-3315-8138-1